Energy components in a lattice of ions and dipoles: Application to the $K(THF)_xC_{24}$ compounds ($x=1,2$)

A. Charlier
Laboratoire de Physique du Solide, Université de Metz, 1 boulevard Arago, 57078 Metz, Cedex 03, France

R. Setton
CRMD/CNRS, 1a rue de la Férollerie, 45071 Orléans, Cedex 2, France

M.-F. Charlier
Laboratoire de Physique du Solide, Université de Metz, 1 boulevard Arago, 57078 Metz, Cedex 03, France
(Received 3 June 1996; revised manuscript received 13 January 1997)

The ion-ion, ion-dipole, and dipole-dipole interaction energies of a three-component crystal lattice are explained and calculated by the Ewald-Kornfeld method, and the relationships thus derived are applied to the $K(THF)_xC_{24}$ ($x=1$ or 2, THF denotes tetrahydrofuran) intercalation compounds of graphite to obtain information on the orientation of the dipolar THF molecules in the lattice. [S0163-1829(97)02923-8]

I. INTRODUCTION

The ternary graphite intercalation compounds (TGIC) $K(THF)_xC_{24}$ (in which THF denotes tetrahydrofuran and $x\approx 1.2$ or 2.2) differ from the simpler binary compounds such as KC_8 and KC_{24} in that they contain a dipolar molecule within the crystal lattice. It is generally admitted that in a binary GIC of the heavy alkali metals (K to Cs), the metal atom is ionized to a large extent and is not covalently bonded to the C atoms, and that its valence electron is delocalized among the C atoms of the two-dimensional (2D) graphitic planes. Even when the third component of a TGIC is a molecule such as C_6H_6 with no intrinsic dipole moment, the presence of the local anisotropic electrostatic field created by the cation and the delocalized countercharge must result in the formation of an induced dipole in the organic molecule, so that the TGIC therefore contains two coexisting lattices, namely, an ionic lattice due to the charge transfer between the metal atom and the carbon (or ''graphene'') layers, and a lattice of dipoles residing on the organic molecules.

One can therefore expect the existence of three components contributing to the energy balance: ion-ion, ion-dipole, and dipole-dipole interactions.

II. THE $K(THF)_xC_{24}$ COMPOUNDS

A. The intercalation compounds

The title compounds were first identified by Nominé and Bonnetain[1] who prepared them by the action of a solution in liquid tetrahydrofuran of the alkali-metal–naphtalene complex on graphite, as shown in the following reaction:

$$K+x(THF)+Npt\rightleftharpoons K^+(THF)_xNpt^-, \tag{2.1}$$

$$K^+(THF)_xNpt^-+nC_g\rightleftharpoons K^+(THF)_xC_n^-+Npt \tag{2.2}$$

(in which Npt stands for naphtalene and C_g stands for graphite). Because the electron affinity of graphite—about equal to its energy of ionization[2] and therefore close to 4.4 eV—is much stronger than that of any other polycondensed aromatic hydrocarbon, the reactions are driven to completion. The fact that the K^+ ion can be solvated by THF molecules thanks to the presence of the two *p* electron pairs on the O atom of the organic molecule is undoubtedly mirrored in the ease of co-intercalation of THF with K. Much work has been done[3] to identify the various products present in the resulting solid mixture, and both *x* and *n* in the above equations have been found to have a range of values that depend on the conditions of preparation. Pure products were prepared by the action of THF vapor on pure, solid KC_{24} as in the reaction[3]

$$KC_{24}+THF(excess)\rightarrow K(THF)_xC_{24}, \tag{2.3}$$

where $x\approx 2.2$. The so-called ''rich'' phase that is formed can lose part of the intercalated THF when submitted to specific conditions of cryopumping to yield a new ''lean'' phase[3,4] with $x\approx 1.2$. Careful *in situ* weight-loss versus time measurements[4–6] allow the isolation of solids with compositions straddling the values $x=2$ or $x=1$, but the compounds with integral stoichiometries do not show any particular features of their physical or chemical properties and, more particularly, of their x-ray diffraction spectra, as compared to those with nonintegral values of *x*, and arguments can be presented indicating that the excess THF with respect to the integral stoichiometry is not adsorbed *on* the solid but is indeed intercalated between the layers.[4]

Both the rich and the lean phase are first-stage compounds. As seen in the values in Table I, the main difference in their structural parameters resides in the distance d_1 separating the graphene layers on either side of the intercalate. The increase in the value of d_1 from 5.42 Å (for the binary KC_{24}) is of course due to the presence of bulky THF molecules in the interlayer space, and the difference in the value of d_1 for the two phases has been traced[3–5] to different orientations of the THF molecules, which have their dipolar axis roughly parallel to the *c* axis in the rich phase, but parallel to the graphene layers in the lean phase. Two possibilities exist for the indexation of the powder diffractogram of the latter, one of them requiring that the *c* parameter be doubled, i.e., that it be characteristic of the height of two

TABLE I. Structural parameters of the ternary compounds. The crystal lattice parameters a, b, c are in Å, with a and b in the graphene layer and c perpendicular to it.

Rich phase	Rich phase	Lean phase
$K(THF)_{2.2}C_{24}$	$[K(THF)_{2.2}C_{24}]_2$	$[K_2(THF)_{2.4}C_{48}]_2$
orthorhombic	monoclinic	monoclinic
$a=7.44$	$a=7.44$	$a=8.53$
$b=8.59$	$b=8.94$	$b=15.39$
$c=8.84$	$c=2(8.91)$	$c=2(7.18)$
	$\gamma=106.10°$	$\gamma=106.10°$

graphene-intercalate-graphene sequences. The indexation of the diffractogram of the lean phase suggests that the ratio C/K is 48/2 rather than 24/1 and, again, that the c parameter be doubled.

A major problem arises in the theoretical calculation of a number of characteristics—such as the Madelung energy—of these and similar compounds that contain components whose stoichiometry is nonintegral. Thus, in the present case, lodging 2.4 molecules of THF on the 2D monoclinic C_{48} lattice of the lean phase (cf. Table I) is impossible, and attempting to eliminate the problem by changing the formula of the compound $[K_2(THF)_{2.4}C_{48}]_2$ to $[K_{20}(THF)_{24}C_{480}]_2$ is senseless since the indexation requires that the 2D lattice contain 48 C atoms, not 480. For the time being, we shall therefore seek a first approximation to the solution by restricting the problem to the compositions $[K_2(THF)_2C_{48}]_2$ for the lean phase and $[K(THF)_2C_{24}]_2$ or $K(THF)_2C_{24}$ for the rich phase.

B. The tetrahydrofuran molecule

Tetrahydrofuran [Figs. 1(a) and 1(b)] is a cyclic ether C_4H_8O, with two pairs of lone p electrons on the oxygen atom. Its geometrical characteristics (Table II) have been determined by electron diffraction[6] and microwave spectroscopy,[7] and since the sum of the internal angles is 540°, the mean conformation of the molecule must be a plane. Its dipole moment p, equal to 1.63 Debye units, is equivalent to 0.54×10^{-29} C m (cf. 1.85 and 1.50 Debye units,[8] respectively for H_2O and NH_3). The center of gravity G^- of the ''free'' negative charges resulting from the presence of the p electrons can be assumed to lie on the O atom, while G^+, that of the corresponding positive countercharge, must be on the C_2 symmetry axis, half-way between lines CE and AB. From the values of the distances and angles in Fig. 1(b) and Table II,

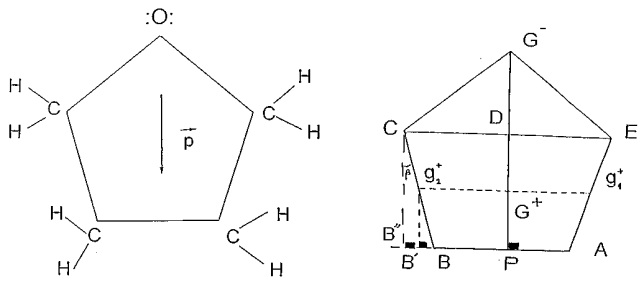

FIG. 1. Tetrahydrofuran molecule. Left figure presents atoms, bonds, and bond angles for THF. The right figure localizes negative center of charge G^- and positive center of charge G^+.

TABLE II. Tetrahydrofuran molecule. Distances are in Å and angles in degrees.

Angles (deg)	Distances (Å)
$\widehat{COC}=111°$	
$\widehat{CCC}=105.5°$	$d_{C\text{-}C}=1.54$
$\widehat{CCH}=127.3°$	$d_{C\text{-}H}=1.10$
$\widehat{HCH}=109.5°$	$d_{C\text{-}O}=1.43$
$\widehat{CCO}=109°$	

$$G^-D=1.43\ \sin[(180°\text{-}111°)/2]=0.810\ \text{Å}$$

and

$$DG^+=[1.54\ \sin[(105.5°)]/2=0.742\ \text{Å},$$

hence

$$G^-G^+=1.552\ \text{Å}.$$

The position of the THF molecules within the crystal lattice is, of course, subject to the steric requirements due to their bulk. After taking into account the van der Waals radii[9] of O ($R_O=1.4$ Å) and H ($R_H=1.2$ Å), the center point of G^-G^+ is found to be coincident (to 0.1 Å) with the center of the sphere circumscribing the THF molecule, and the positive end of the vector attached to the dipole moment of THF can therefore be placed thereon with sufficient accuracy.

III. THE INTERACTION ENERGY COMPONENTS

A. Madelung energy of the binary compound KC_{24}

A test computation performed using the relationships (A3) in Appendix A yielded correct values for the Madelung[10–16] energy E_M and the Madelung constant for CsCl, namely, $E_M=-7.108$ eV and $a=1.7626$, respectively, in agreement with the commonly accepted values.

Although the binary potassium derivative KC_{24} featured in Eq. (2.3) is a second-stage intercalation compound, the ternary derivative that is formed is first stage, so that the reaction described by Eq. (2.3) can, at least formally, be broken down into two successive steps, namely,

$$KC_{24}(\text{second stage})\rightleftharpoons[KC_{24}(\text{first stage})] \qquad (3.1)$$

followed by

$$[KC_{24}(\text{first stage})] + \text{THF(excess)}\rightleftharpoons K(THF)_xC_{24}(\text{first stage}) \qquad (3.2)$$

in which the square brackets denote the hypothetical formation of a first-stage compound. One should also remember that the local density of occupation of the alkali-metal ions changes in the course of reactions (3.1) and (3.2), with K/C being 1/12 for the second stage and 1/24 for the first stage. Combined with the change in distance between the graphene layers on either side of the intercalated layer, this results in

TABLE III. Ion-ion interaction (Madelung energy) in eV of some hypothetical K-graphite intercalation compounds. All distances are in Å. The Madelung energy values refer to compounds with crystal lattice parameters equal to those given at the head of the column, except for the value of d_1 (the distance between the graphene layers on either side of the intercalated ion) given at the beginning of the line. In all cases, the positive metal ion is exactly halfway between the adjacent layers. Values in *italics* correspond to hypothetical *binary derivatives* with the same crystal lattice as the ternary K-THF-graphite compounds. All the values are normalized with respect to a single K atom.

	Structural characteristics			
	KC_{24} Hexagonal	KC_{24} Orthorhombic	$[KC_{24}]_2$ Monoclinic	$[K_2C_{48}]_2$ Monoclinic
	$a=8.53$	$a=7.44$	$a=7.44$	$a=8.53$
	$b=8.53$	$b=8.59$	$b=8.94$	$b=15.39$
	$c=5.42$	$c=8.84$	$c=2(8.91)$	$c=2(7.18)$
			$\gamma=106.10$	$\gamma=106.10$
Madelung (ion-ion) energy				
$d_1=5.42$	−2.207	−2.161	−2.166	−2.053
$d_1=7.18$	−1.657	−1.620	−1.625	*−1.558*
$d_1=8.84$	−1.078	*−1.045*	−1.049	−1.001
$d_1=8.91$	−1.053	−1.020	*−1.024*	−0.977

an important modification of the Madelung energy, as seen in the values given in Table III for some real and hypothetical KC_{24} compounds, the latter corresponding to structures with crystal lattices whose characteristics are those of the ternary compounds. The evaluations were performed assuming that the charge transfer from the K atom to the graphene layers is complete,[17] with the ion halfway between the adjacent graphene layers. The values in Table III show that the parameter with the greatest influence on the energy is d_1 (the distance between the graphene layers on either side of the intercalated species), rather than the characteristics of the 2D lattice in which the average distance between first-neighbor K^+ ions is nearly the same. Similarly, the influence of the C/K ratio on E_M can be gauged by comparison with the corresponding values of E_M for the ''saturated'' (i.e., richest) first-stage compound $(KC_8)_n$ for which the stacking $A\alpha$, corresponding to $n=1$, gives $E_M=-2.416$ eV, while the stacking $A\alpha A\beta A\gamma A\delta$, which corresponds to $n=4$, yields $E_M=-2.424$ eV, both structures[18,19] having $d_1=5.42$ Å.

B. Ion↔dipole and dipole interactions in the ternary compounds

The heat of sublimation[20] S of the hydrogen chloride HCL molecule is 4.5 kcal. It is connected to reticular energy of a system of dipoles of equal moment $p=1.08$ Debye. By using the model of Born given by Kornfeld in Ref. 20 (a cube of side $\delta/2$ obtained with the help of two regular congruent tetrahedrons), the dipoles are located on the four diagonals of the cube. In a volume δ^3 one counts 8 dipoles. Energy $E_{\text{dip-dip}}$ computed by our formula (B9) gives the value -443×10^{-18} kcal/mole. Kornfeld's formula $S=-1.565\times10^{-8}NE_{\text{dip-dip}}$, where N is Avogadro's number, provides a good value for the energy of sublimation $S=4.174$ kcal/mole and validates our formula (B9).

It is convenient to use the system of spherical coordinates. The projection of the dipole on the a,b plane of the crystal lattice forms an angle θ (the longitude) with a, while the angle between the dipole and c is φ (the colatitude). With this notation, the dipoles parallel to the graphene axis in the lean phase all have $\varphi=\pi/2$ whereas $\varphi=0$ for those whose dipolar axis is parallel to the c axis.

Figure 2 shows possible configurations for the dipoles and the metal ions in a single intercalate layer of the lean phase and the rich phases, i.e., for the $K_2(THF)_2$ and $K(THF)_2$ moieties, respectively. Since the structural parameter c requires that d_1 be doubled for the lean phase, the four layouts A–D in Fig. 2 give the six possible combinations of nonidentical successive layers shown in Table IV, in which θ_1 and θ_2 are the longitudes of the dipoles in one of the intercalate layers and θ_3 and θ_4 are the orientations of the dipoles in the other layer. As regards the monoclinic rich phase in which two nonidentical layers of the intercalate must also be superposed along the c axis, the dipoles in the layout E can give rise to the four different combinations given in the second part of Table IV, whereas there are only two possibilities of configuring the two dipoles in F, which corresponds to the intercalate of the orthorhombic rich phase.

For each of the three sections in Table IV, the configuration placed at the head of the list stands out as being apparently much more favorable than the others since it corresponds to the lowest value of the sum $E_{\text{ion}\leftrightarrow\text{dip}}+E_{\text{dip-dip}}$ namely, −0.8514 eV (lean phase, monoclinic), −0.4722 eV

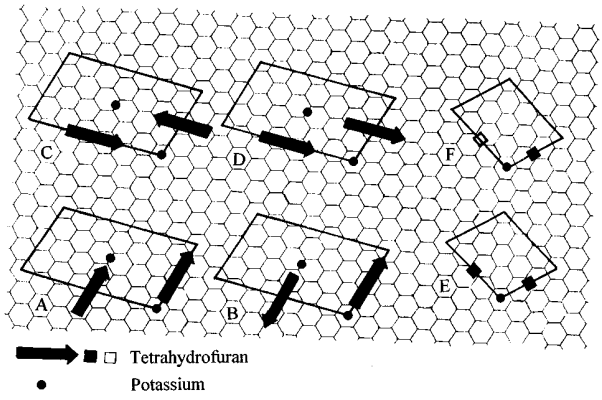

FIG. 2. Possible configurations for the dipoles and metal ions. Different positions of the THF dipoles and the K ions in a single intercalate layer for the lean and rich phases are shown.

TABLE IV. Ion↔dipole and dipole-dipole components (in eV) of the total interaction energy. Various possible configurations of the dipoles in the rich and lean phases are given; for each phase, the composition indicated is that used in the calculation (see text).

Lean phase, $[K_2(THF)_2C_{48}]_2$, monoclinic, $-E_{\text{ion-ion}}=1.558$ eV

θ_1	θ_2	θ_3	θ_4	$-E_{\text{ion}\leftrightarrow\text{dip}}$	$-E_{\text{dip-dip}}$	−sum
0	0	γ	$\gamma+\pi$	0.8160	0.0354	0.8514
0	π	γ	$\gamma+\pi$	0.6732	0.0026	0.6758
0	0	$\gamma+\pi$	$\gamma+\pi$	0.3822	0.0845	0.4667
0	π	$\gamma+\pi$	$\gamma+\pi$	0.2415	0.0455	0.2870
γ	$\gamma+\pi$	$\gamma+\pi$	$\gamma+\pi$	0.1852	0.0382	0.2234
0	0	0	π	0.1321	0.0426	0.1747

Rich phase, structure $K(THF)_2C_{24}$, orthorhombic, $-E_{\text{ion-ion}}=1.045$ eV

φ_1	φ_2	$-E_{\text{ion}\leftrightarrow\text{dip}}$	$-E_{\text{dip-dip}}$	−sum
0	0	0.4046	0.0676	0.4722
0	π	0.1649	0.0401	0.2050

Rich phase, structure $[K(THF)_2C_{24}]_2$, monoclinic, $-E_{\text{ion-ion}}=1.024$ eV

φ_1	φ_2	φ_3	φ_4	$-E_{\text{ion}\leftrightarrow\text{dip}}$	$-E_{\text{dip-dip}}$	−sum
0	0	0	π	0.5137	0.0325	0.5462
0	0	π	0	0.4547	0.0325	0.4872
0	π	π	0	0.4210	0.0306	0.4516
0	0	π	π	0.1864	0.0367	0.2231

(rich phase, orthorhombic), and -0.5462 eV (rich phase, monoclinic). When added to the appropriate values of $E_{\text{ion-ion}}$ from Table III, the total interaction energies are found to be

lean phase, $[K_2(THF)_2C_{48}]_2$, monoclinic, $E_{\text{interaction}}=-2.409$ eV,

rich phase, $K(THF)_2C_{24}$, orthorhombic, $E_{\text{interaction}}=-1.517$ eV,

rich phase, $[K(THF)_2C_{24}]_2$, monoclinic, $E_{\text{interaction}}=-1.570$ eV

and the most likely configurations for the dipoles are $\theta_1=0$, $\theta_2=0$, $\theta_3=\gamma$, $\theta_4=\gamma+\pi$ for the monoclinic lean phase, $\varphi_1=0$, $\varphi_2=0$, $\varphi_3=0$, $\varphi_4=\pi$ for the monoclinic rich phase, and $\varphi_1=0$, $\varphi_2=0$ for the orthorhombic rich phase.

We assumed in our calculations rigid dipoles in an unrelaxed lattice but our method is adapted to optimum geometry determination. Orientations are calculated for THF molecules in three specified lattices, under the assumption that the internal geometry and dipole moment of the THF molecules are independent of the local environment. A minimalization of the total energy, taking into account a possible variation of the dipole moment value, has been performed for p near to 1.63 Debye. For the different dipole and ion configurations studied here, the numerical value of p is slightly lower than 1.63 but the difference never exceeds 3%. The authors believe that it is possible to determine the optimum geometry for other lattices of ions and dipoles than $K(THF)_xC_{24}$ compounds with this method. Unfortunately in our case the number of parameters for the minimalization of energy is too high: stoichiometry and lattice parameters, positions and orientations of the dipoles, dipole moment value, charge transfer, etc.

IV. CONCLUSIONS

The Kornfeld extension[20] of the Madelung-Ewald method to dipole-containing ionic solids can provide useful information concerning the configuration of the dipoles within the lattice, in spite of the fact that the present lack of adequate experimental thermodynamic data on ternary intercalation compounds of graphite unfortunately prevents any comparison of the results with known numerical values. A full exploitation of the method would, however, require taking into account the nonintegral values of the tetrahydrofuran/potassium ratio, a problem for which no adequate solution has yet been found.

APPENDIX A: ION-ION INTERACTION (OR MADELUNG) ENERGY

The Ewald method of computation of the ion-ion interaction is well known.[21–24] Consider a crystalline solid sufficiently extensive that anisotropy effects due to the proximity of the surface can be neglected, and let O be the origin to which the three crystal axes of the elementary cell parallelepiped are referred. The position of an ion I in the cth cell of the solid can be fully described by the vector $\mathbf{OI}$, viz., $\mathbf{OI}=\mathbf{OO'}+\mathbf{O'I}=\mathbf{c}+\mathbf{i}=\mathbf{I}$, in which $\mathbf{c}$ is a vector localizing the elementary cell with respect to the origin and $\mathbf{i}$ is a vector giving the position of I within the cell. The position vector $\mathbf{r}=\mathbf{OM}$ attached to any point M within the whole lattice characterizes the position of M with respect to the origin O. Hence, the electrostatic potential at M due to all the ions in the crystal lattice is

$$V_{\text{ion}}(M)=\sum_{\mathbf{i}}\sum_{\mathbf{c}}\frac{q_i}{4\pi\epsilon_0\|\mathbf{r}-\mathbf{c}-\mathbf{i}\|}, \tag{A1}$$

i.e.,

$$V_{\text{ion}}(M)=\frac{1}{2\pi^{3/2}\epsilon_0}\sum_{\mathbf{I}} q_I\int_0^H e^{-\|\mathbf{r}-\mathbf{I}\|^2\lambda^2}d\lambda + \frac{1}{4\pi\epsilon_0}\sum_{\mathbf{I}} q_I\frac{1}{\|\mathbf{r}-\mathbf{I}\|}\text{erfc}(\|\mathbf{r}-\mathbf{I}\|H), \tag{A2}$$

where erfc is the *complementary error function.* The total ion-ion or Madelung energy of the crystal lattice, noted here $E_{\text{ion-ion}}$, is therefore

$$E_{\text{ion-ion}}=\frac{1}{2\tau\epsilon_0}\sum_{\mathbf{I}}\sum_{\mathbf{I'}}\sum_{\mathbf{h}\neq\mathbf{0}} q_{I'}q_I e^{i\mathbf{h}\cdot(\mathbf{I'}-\mathbf{I})}\frac{e^{-h^2/4H^2}}{h^2} + \frac{1}{8\pi\epsilon_0}\sum_{\mathbf{I},\mathbf{I}\neq\mathbf{I'}}\sum_{\mathbf{I'}}\frac{q_I q_{I'}}{\|\mathbf{I'}-\mathbf{I}\|}\text{erfc}(\|\mathbf{I'}-\mathbf{I}\|H) - \frac{H}{4\pi^{3/2}\epsilon_0}\sum_{\mathbf{i}} q_i^2. \tag{A3}$$

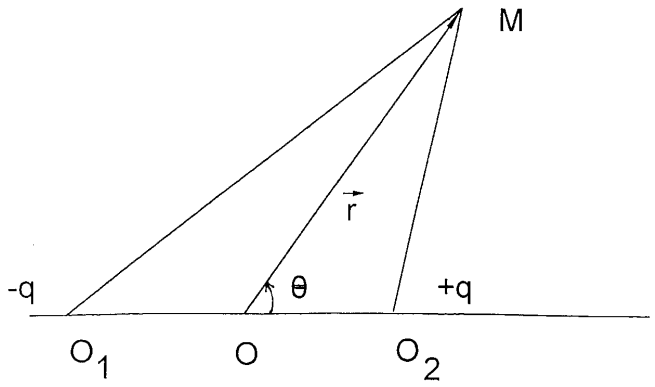

FIG. 3. Dipole. We define position and orientation of the THF dipole relative to the origin of the lattice.

h is a reciprocal vector.[25,26] Although the parameter H can be chosen quite arbitrarily because it should normally not affect the final result, experience shows that the necessary truncation of the series in (A3) introduces errors since too small (or too large) a value of H will favor the rapid convergence of one (or the other) series. Procedures exist[27] to determine the best value of H, i.e., that value that will give the same order of magnitude for the two residues—which are of opposite sign—of the series.

APPENDIX B: DIPOLE-DIPOLE INTERACTION ENERGY

The procedure yielding the energy contribution of a lattice of dipoles with given orientation and intensity characteristics is similar to that used by Kornfeld,[20,28,29] de Wette and Schacher,[30] and Nijboer.[31]

In Fig. 3, the charges $-q$ and $+q$ respectively at O_1 and O_2 constitute a dipole D whose moment $\mathbf{p}_D = q\mathbf{l}$ involves the vector $\mathbf{l}$ characteristic of the relative orientation and distance between O_1 and O_2. The position of the midpoint of $\mathbf{l}$ with respect to the origin is given by the vector D such that $\mathbf{D} = \mathbf{c} + \mathbf{d}$ in which $\mathbf{d}$ is the vector describing the position and orientation of the dipole with respect to the origin of the lattice within which D is placed, and $\mathbf{c}$ localizes the lattice itself with respect to the origin O.

At a point M, the dipole creates a potential $v(M)$, which is

$$v(M) = \frac{\mathbf{p}_D \cdot \mathbf{r}}{4\pi\epsilon_0 r^3}. \tag{B1}$$

In order to be able to retain the formalism developped in Appendix A for pointlike charges, it is convenient to define an operator $d/d\mathbf{p}$ as

$$\frac{d}{d\mathbf{p}} = -\frac{\mathbf{p}\cdot\mathbf{r}}{r}\frac{d}{dr} \tag{B2}$$

from which it follows that

$$v(M) = \frac{d}{d\mathbf{p}}\left(\frac{1}{4\pi\epsilon_0 r}\right) \tag{B3}$$

and, since the vector between D and M is $\mathbf{DM} = \mathbf{r} - \mathbf{D}$, then the potential at M due to all the dipoles in the lattice is

$$V_{\text{dip}}(M) = \sum_{\mathbf{D}} \frac{d}{d\mathbf{p}_D}\left(\frac{1}{4\pi\epsilon_0\|\mathbf{r}-\mathbf{D}\|}\right). \tag{B4}$$

Using now

$$\frac{1}{4\pi\epsilon_0\|\mathbf{r}-\mathbf{D}\|} = \frac{1}{2\pi^{3/2}\epsilon_0}\int_0^H e^{-\|\mathbf{r}-\mathbf{D}\|^2\lambda^2} d\lambda + \frac{1}{4\pi\epsilon_0\|\mathbf{r}-\mathbf{D}\|}\operatorname{erfc}(\|\mathbf{r}-\mathbf{D}\|H) \tag{B5}$$

the expression (B4) can be modified to

$$V_{\text{dip}}(M) = -\frac{i}{\epsilon_0\tau}\sum_{\mathbf{D}}\sum_{\mathbf{h}\neq\mathbf{0}} (\mathbf{p}_D\cdot\mathbf{h})\frac{e^{-h^2/4H^2}}{h^2} e^{i\mathbf{h}\cdot(\mathbf{r}-\mathbf{D})} + \frac{1}{4\pi\epsilon_0}\sum_{\mathbf{D}}\frac{\mathbf{p}_D\cdot(\mathbf{r}-\mathbf{D})}{\|\mathbf{r}-\mathbf{D}\|^3}\operatorname{erfc}(\|\mathbf{r}-\mathbf{D}\|H) + \frac{H}{2\pi^{3/2}\epsilon_0}\sum_{\mathbf{D}}\frac{\mathbf{p}_D\cdot(\mathbf{r}-\mathbf{D})}{\|\mathbf{r}-\mathbf{D}\|^2} e^{-\|\mathbf{r}-\mathbf{D}\|^2H^2}. \tag{B6}$$

The potential $V'_{\text{dip}}(M)$ at M due to all the dipoles except a dipole D' is therefore

$$V'_{\text{dip}}(M) = -\frac{i}{\epsilon_0\tau}\sum_{\mathbf{D}\neq\mathbf{D}'}\sum_{\mathbf{h}\neq\mathbf{0}} (\mathbf{p}_D\cdot\mathbf{h})\frac{e^{-h^2/4H^2}}{h^2} e^{i\mathbf{h}\cdot(\mathbf{r}-\mathbf{D})} + \frac{1}{4\pi\epsilon_0}\sum_{\mathbf{D}\neq\mathbf{D}'}\frac{\mathbf{p}_D\cdot(\mathbf{r}-\mathbf{D})}{\|\mathbf{r}-\mathbf{D}\|^3} - \frac{1}{4\pi\epsilon_0}\sum_{\mathbf{D}\neq\mathbf{D}'}\sum\frac{\mathbf{p}_D\cdot(\mathbf{r}-\mathbf{D})}{\|\mathbf{r}-\mathbf{D}\|^3}\operatorname{erf}(\|\mathbf{r}-\mathbf{D}\|H) + \frac{H}{2\pi^{3/2}\epsilon_0}\sum_{\mathbf{D}\neq\mathbf{D}'}\frac{\mathbf{p}_D\cdot(\mathbf{r}-\mathbf{D})}{\|\mathbf{r}-\mathbf{D}\|^2} e^{-\|\mathbf{r}-\mathbf{D}\|^2H^2}, \tag{B7}$$

which yields, for the dipole-dipole interaction energy

$$E_{\text{dip-dip}} = \frac{1}{2}\sum_{\mathbf{D}'} \mathbf{p}_{D'}\cdot\boldsymbol{\nabla} V'_{\text{dip}}(D'), \tag{B8}$$

or, explicitly,

$$E_{\text{dip-dip}}=\frac{1}{2\epsilon_0\tau}\sum_{\mathbf{D}}\sum_{\mathbf{D}'\neq\mathbf{D}}\sum_{\mathbf{h}\neq\mathbf{0}}(\mathbf{p}_D\cdot\mathbf{h})(\mathbf{p}_{D'}\cdot\mathbf{h})\frac{e^{-h^2/4H^2}}{h^2}e^{i\mathbf{h}\cdot(\mathbf{D}'-\mathbf{D})}-\frac{1}{4\pi\epsilon_0}\sum_{\mathbf{D}}\sum_{\mathbf{D}'\neq\mathbf{D}}\frac{\mathbf{p}_D\cdot(\mathbf{D}'-\mathbf{D})\mathbf{p}_{D'}\cdot(\mathbf{D}'-\mathbf{D})}{\|\mathbf{D}'-\mathbf{D}\|^5}$$
$$\times\operatorname{erfc}(\|\mathbf{D}'-\mathbf{D}\|H)-\frac{H}{2\pi^{3/2}\epsilon_0}\sum_{\mathbf{D}}\sum_{\mathbf{D}'\neq\mathbf{D}}\frac{\mathbf{p}_D\cdot(\mathbf{D}'-\mathbf{D})\mathbf{p}_{D'}\cdot(\mathbf{D}'-\mathbf{D})}{\|\mathbf{D}'-\mathbf{D}\|^4}e^{-\|\mathbf{D}'-\mathbf{D}\|^2H^2}$$
$$-\frac{H^3}{2\pi^{3/2}\epsilon_0}\sum_{\mathbf{D}}\sum_{\mathbf{D}'\neq\mathbf{D}}\frac{\mathbf{p}_D\cdot(\mathbf{D}'-\mathbf{D})\mathbf{p}_{D'}\cdot(\mathbf{D}'-\mathbf{D})}{\|\mathbf{D}'-\mathbf{D}\|^2}e^{-\|\mathbf{D}'-\mathbf{D}\|^2H^2}. \tag{B9}$$

Note that the relationships in Eq. (B9) are symmetrical in $\mathbf{D}$ and $\mathbf{D}'$, and that the sum $\Sigma_{\mathbf{D}}\mathbf{p}_D\cdot\mathbf{h}e^{i\mathbf{h}\cdot\mathbf{D}}$ plays the same role as the structure factor $F_{\text{ion}}(\mathbf{h})=\Sigma_{\mathbf{i}}q_ie^{-i\mathbf{h}\cdot\mathbf{i}}$ in Eq. (A3). Again, the interaction energy $E_{\text{dip-dip}}$ is, at least in principle, independent of H and only dependent on the relative position vector $\mathbf{D}-\mathbf{D}'$ and on the moments $\mathbf{p}_D$ and $\mathbf{p}_{D'}$.

APPENDIX C: MUTUAL ION-DIPOLE INTERACTION ENERGY

There are, in fact, two components of the mutual interaction energy $E_{\text{ion}\leftrightarrow\text{dip}}$ between ions and dipoles, namely, the energy due to the presence of ions in the potential field created by the lattice of dipoles, and the energy due to the presence of the dipoles in the potential field created by the ions. The relationship

$$E_{\text{ion-dip}}=\sum_{\mathbf{D}}\mathbf{p}_D\cdot\boldsymbol{\nabla}V_{\text{ion}}(D) \tag{C1}$$

yields the ion-dipole interaction energy

$$E_{\text{ion-dip}}=\frac{i}{\epsilon_0\tau}\sum_{\mathbf{h}\neq\mathbf{0}}\sum_{\mathbf{c}}\sum_{\mathbf{D}}F_{\text{ion}}(\mathbf{h})e^{i\mathbf{h}\cdot(\mathbf{D}-\mathbf{c})}\frac{e^{-h^2/4H^2}}{h^2}\mathbf{p}_D\cdot\mathbf{h}$$
$$-\frac{1}{4\pi\epsilon_0}\sum_{\mathbf{I}}\sum_{\mathbf{D}}q_I\frac{\mathbf{p}_D\cdot(\mathbf{D}-\mathbf{I})}{\|\mathbf{D}-\mathbf{I}\|^3}\operatorname{erfc}(\|\mathbf{D}-\mathbf{I}\|H)$$
$$-\frac{H}{2\pi^{3/2}\epsilon_0}\sum_{\mathbf{I}}\sum_{\mathbf{D}}q_I\frac{\mathbf{p}_D\cdot(\mathbf{D}-\mathbf{I})}{\|\mathbf{D}-\mathbf{I}\|^2}e^{-\|\mathbf{D}-\mathbf{I}\|^2H^2}. \tag{C2}$$

$E_{\text{ion-dip}}$ is a complex number, as witnessed by the presence of i before the treble sum. As will be seen below, the addition of $E_{\text{dip-ion}}$, the dipole-ion interaction energy, renders the sum of these two interaction energies real.

The potential at M due to the dipole lattice is, as given in Appendix B,

$$V_{\text{dip}}(M)=-\frac{i}{\epsilon_0\tau}\sum_{\mathbf{D}}\sum_{\mathbf{h}\neq\mathbf{0}}(\mathbf{p}_D\cdot\mathbf{h})\frac{e^{-h^2/4H^2}}{h^2}e^{i\mathbf{h}\cdot(\mathbf{r}-\mathbf{D})}$$
$$+\frac{1}{4\pi\epsilon_0}\sum_{\mathbf{D}}\frac{\mathbf{p}_D\cdot(\mathbf{r}-\mathbf{D})}{\|\mathbf{r}-\mathbf{D}\|^3}\operatorname{erfc}(\|\mathbf{r}-\mathbf{D}\|H)$$
$$+\frac{H}{2\pi^{3/2}\epsilon_0}\sum_{\mathbf{D}}\frac{\mathbf{p}_D\cdot(\mathbf{r}-\mathbf{D})}{\|\mathbf{r}-\mathbf{D}\|^2}e^{-\|\mathbf{r}-\mathbf{D}\|^2H^2} \tag{C3}$$

and since

$$E_{\text{dip-ion}}=\sum_{\mathbf{I}}q_IV_{\text{dip}}(I) \tag{C4}$$

then

$$E_{\text{dip-ion}}=-\frac{i}{\epsilon_0\tau}\sum_{\mathbf{D}}\sum_{\mathbf{h}\neq\mathbf{0}}\sum_{\mathbf{I}}q_I(\mathbf{p}_D\cdot\mathbf{h})\frac{e^{-h^2/4H^2}}{h^2}e^{i\mathbf{h}\cdot(\mathbf{I}-\mathbf{D})}$$
$$+\frac{1}{4\pi\epsilon_0}\sum_{\mathbf{D}}\sum_{\mathbf{I}}q_I\frac{\mathbf{p}_D\cdot(\mathbf{I}-\mathbf{D})}{\|\mathbf{I}-\mathbf{D}\|^3}\operatorname{erfc}(\|\mathbf{I}-\mathbf{D}\|H)$$
$$+\frac{H}{2\pi^{3/2}\epsilon_0}\sum_{\mathbf{D}}\sum_{\mathbf{I}}q_I\frac{\mathbf{p}_D\cdot(\mathbf{I}-\mathbf{D})}{\|\mathbf{I}-\mathbf{D}\|^2}e^{-\|\mathbf{I}-\mathbf{D}\|^2H^2}. \tag{C5}$$

The sum of (C2) and (C5) is the total or mutual ion-dipole interaction energy

$$E_{\text{ion}\leftrightarrow\text{dip}}=E_{\text{ion-dip}}+E_{\text{dip-ion}}$$
$$=-\frac{2}{\epsilon_0\tau}\sum_{\mathbf{h}\neq\mathbf{0}}\sum_{\mathbf{I}}\sum_{\mathbf{D}}q_I\sin[\mathbf{h}\cdot(\mathbf{D}-\mathbf{I})]\frac{e^{-h^2/4H^2}}{h^2}\mathbf{p}_D\cdot\mathbf{h}$$
$$-\frac{1}{2\pi\epsilon_0}\sum_{\mathbf{I}}\sum_{\mathbf{D}}q_I\frac{\mathbf{p}_D\cdot(\mathbf{D}-\mathbf{I})}{\|\mathbf{D}-\mathbf{I}\|^3}\operatorname{erfc}(\|\mathbf{D}-\mathbf{I}\|H)$$
$$-\frac{H}{\pi^{3/2}\epsilon_0}\sum_{\mathbf{I}}\sum_{\mathbf{D}}q_I\frac{\mathbf{p}_D\cdot(\mathbf{D}-\mathbf{I})}{\|\mathbf{D}-\mathbf{I}\|^2}e^{-\|\mathbf{D}-\mathbf{I}\|^2H^2} \tag{C6}$$

in which the sine term arises from the difference in sign of the $(\mathbf{I}-\mathbf{D})$ factor in the exponent. The total interaction energy for the lattice of ions and dipoles is the sum of the expressions in (A3), (B9), and (C6), namely,

$$E=E_{\text{ion-ion}}+E_{\text{dip-dip}}+E_{\text{ion}\leftrightarrow\text{dip}}. \tag{C7}$$

[1] M. Nominé and L. Bonnetain, C.R. Acad. Sci. Ser. C **264**, 2084 (1967).
[2] A. Braun and G. Bush, Helv. Phys. Acta **20**, 33 (1947).
[3] F. Beguin, Ph.D. thesis, University of Orléans (France), 1980.
[4] R. Setton in *Graphite Intercalation I*, edited by H. Zabel and S.A. Solin (Springer-Verlag, Berlin, 1990), pp. 313–327.
[5] M.F. Quinton, A.P. Legrand, and F. Béguin, Synth. Met. **14**, 179 (1986).
[6] J.Y. Beach, J. Chem. Phys. **9**, 54 (1941).
[7] K. Murty and Sree Rama (unpublished).
[8] *CRC Handbook of Chemistry and Physics*, 61st ed., edited by R.C. Weast (CRC Press, Boca Raton, FL, 1980–81), p. E64.
[9] A. Bondi, J. Phys. Chem. **68**, 441 (1964).
[10] E. Madelung, Phys. Z. **19**, 524 (1918).
[11] H.M. Evjen, Phys. Rev. **39**, 675 (1932).
[12] K. Hoejendahl, K. Dan. Vidensk. Selsk. Math.-Fys. Medd. **16**, 138 (1938).
[13] F.C. Frank, Philos. Mag. **41**, 1287 (1950).
[14] F. Bertaut, J. Phys. Radium **13**, 499 (1952).
[15] D.H. Templeton, J. Chem. Phys. **23**, 1629 (1955).
[16] J.O. Banos, thesis, University of Aix-Marseille, France, 1984.
[17] G.P. Carver, Phys. Rev. B **2**, 2284 (1970).
[18] R. Setton, Synth. Met. **34**, 279 (1989).
[19] R.M. Metzger, Mol. Cryst. Liq. Cryst. **85**, 97 (1982).
[20] H. Kornfeld, thesis, Goettingen (Germany), 1923.
[21] P.P. Ewald, Ann. Phys. (Leipzig) **64**, 253 (1921).
[22] P.P. Ewald, Goettinger Nachr., Math.-Phys. Kl. II **3**, 55 (1937).
[23] P. Epstein, Math. Ann. **56**, 615 (1903).
[24] P. Epstein, Math. Ann. **63**, 205 (1907).
[25] W.A. Harrison, *Electronic Structure and the Properties of Solids* (Freeman, San Francisco, 1980), p. 304.
[26] C. Kittel, *Introduction to Solid State Physics*, 3rd ed. (Wiley, New York, 1967), p. 53.
[27] D. Bonnin and A.P. Legrand, Chem. Phys. Lett. **30**, 296 (1975).
[28] M. Born and H. Kornfeld, Phys. Z. **24**, 121 (1923).
[29] M. Born, *Dynamik der Kristallgitter* (Tuebner, Leipzig, 1915).
[30] F.W. de Wette and G.E. Schacher, Phys. Rev. A **37**, A78 (1965).
[31] B. R. A. Nijboer, Phys. **23**, 309 (1957).